



Establishment of a human cell line stably overexpressing mouse Nip45 and characterization of Nip45 subcellular localization

Kohtaro Hashiguchi^a, Masumi Ozaki^a, Isao Kuraoka^b, Hisato Saitoh^{a,c,d,*}

^a Department of Biological Sciences, Graduate School of Science and Technology, Kumamoto University, Kumamoto, Japan

^b Biological Chemistry Group, Division of Chemistry, Graduate School of Engineering Science, Osaka University, Osaka, Japan

^c Department of New Frontier Sciences, Graduate School of Science and Technology, Kumamoto University, Kumamoto, Japan

^d Global COE (Centers of Excellence) Program, Global Initiative Center for Pulsed Power Engineering, Kumamoto University, Kumamoto, Japan

ARTICLE INFO

Article history:

Received 2 November 2012

Available online 15 November 2012

Keywords:

Nip45

SUMO

Ubc9

Proteasome

PML bodies

ABSTRACT

The nuclear factor of activated T cells, cytoplasmic, calcineurin dependent 2 interacting protein, Nfatc2ip (Nip45), has been implicated as a crucial coordinator of the immune response and of cellular differentiation in humans and mice, and contains SUMO-like domains in its C-terminal region. However, the significance of its N-terminal region and its correlation to the SUMO modification pathway remain largely uncharacterized. In this study, a human cultured cell line was established, in which FLAG-tagged mouse Nip45 (FLAG-mNip45) was stably overexpressed. Under standard, non-stressful conditions, we detected FLAG-mNip45 diffusely distributed in the nucleus. Intriguingly, proteasome inhibition by MG132 caused FLAG-mNip45, together with SUMOylated proteins, to localize in nuclear domains associated with promyelocytic leukemia protein. Finally, using an *in vitro* binding assay, we showed interaction of the N-terminal region of mNip45 with both free SUMO-3 and SUMO-3 chains, indicating that Nip45 may, in part, exert its function via interaction with SUMO/SUMOylated proteins. Taken together, our study provides novel information on a poorly characterized mammalian protein and suggests that our newly established cell line will be useful for elucidating the physiological role of Nip45.

© 2012 Elsevier Inc. All rights reserved.

1. Introduction

Nip45 was originally identified as ‘nuclear factor of activated T cells (NFAT) interacting protein of 45-kDa’, a co-regulator with NFAT and the T helper 2 (Th2)-specific transcription factor, c-Maf, to induce IL-4 production [1]. It has also recently been shown to regulate members of the tumor necrosis factor (TNF)-receptor-associated factor (TRAF) family of proteins and has thus been implicated in the immune response [2–5] and cellular differentiation, such as receptor activator of NF-κB ligand (RANKL)-mediated osteoclast differentiation [6]. This protein can also recruit protein arginine N-methyltransferase 1 (PRMT1) to facilitate NFAT-driven transcriptional activity [7]. These data thus suggest that Nip45 is a multi-functional protein involved in multiple cellular signal transduction pathways, such as TNF-TRAF, RANKL-RANK, Toll and NF-κB pathways, indicating it as a potential therapeutic target for cancer and other human diseases. However, the molecular details of how Nip45 interacts with seemingly distinct signaling pathways remain largely unknown.

* Corresponding author at: Department of Biological Sciences, Graduate School of Science and Technology, Kumamoto University, Kumamoto, Japan. Fax: +81 96 342 3450.

E-mail address: hisa@kumamoto-u.ac.jp (H. Saitoh).

Amino acid sequence comparison identified Nip45 as a member of the Rad60-Esc2-Nip45 (RENI) protein family, which is conserved from yeast to humans [8]. RENI family members are distinguished from other protein families by their tripartite (bipartite for plant homologs) domain architecture. An N-terminal polar/charged low-complexity segment and two consecutive unique small ubiquitin-related modifier (SUMO)-like domains, referred to as SLDs, in the C-terminal region can be detected by sequence-based domain and fold-recognition methods as well as by a structure-based similarity method [8]. For instance, mouse and human Nip45 proteins (mNip45 and hNip45) consist of 421 and 419 amino acid residues, respectively, and show 71% identity (79% similarity) with each other over their entire polypeptide sequences. Both contain two SLDs in their C-terminal regions: the N-terminal and C-terminal domains of the C-terminal region are designated as SLD1 and SLD2, respectively (see Fig. 1A). Polypeptide sequence comparison of mNip45-SLD1 versus hNip45-SLD1 shows 90% identity (96% similarity), and a comparison of their SLD2s shows 92% identity (95% similarity). The N-terminal regions of both mNip45 and hNip45 contain an excess of polar/charged residues and have only 60% identity (68% similarity) with a low complexity, implying that these regions are most likely distinct from the C-terminal SLDs and are conformationally flexible segments without inherent structural preference [9,10].

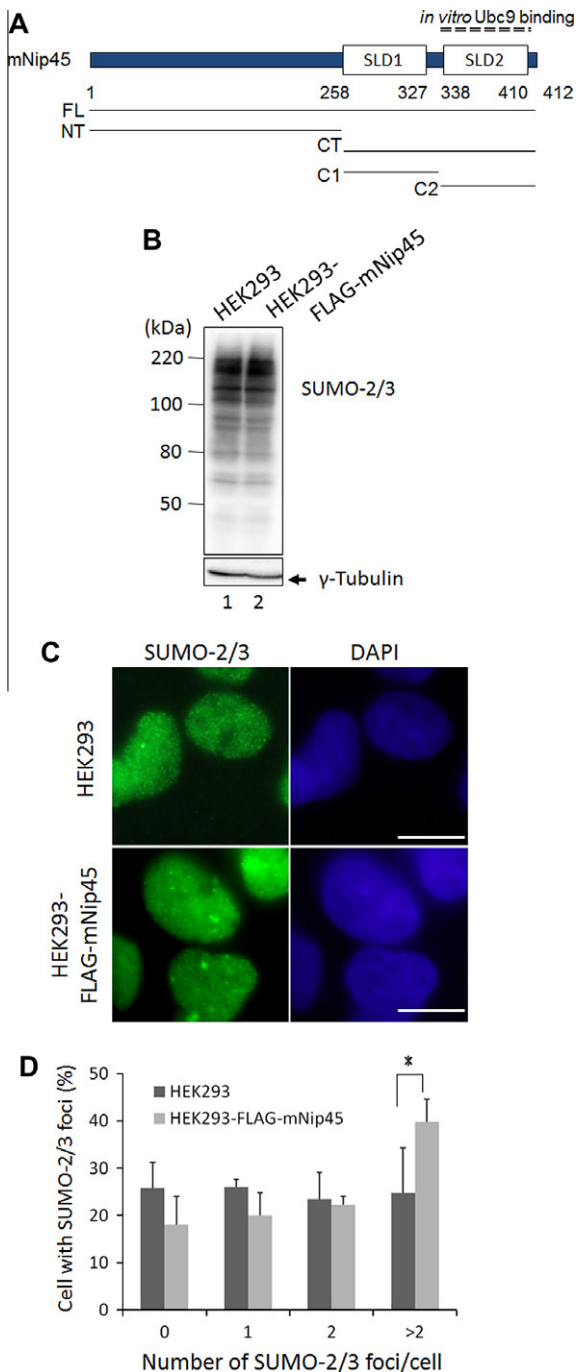


Fig. 1. Detection of SUMO/SUMOylated proteins in FLAG-mNip45 expressing cells. (A) Schematic representation of mNip45. The numbers correspond to the amino acid residues in mNip45. The positions of the SUMO-like domains (SLD1 and SLD2) are shown [11]. The full length (FL), N-terminal (NT), C-terminal (CT), SLD1-containing (C1), and SLD2-containing (C2) domain constructs used in this study are represented as thin black lines. (B) Non-transfected HEK293 cells (–: lane 1) and FLAG-mNip45 expressing cells (+: lane 2) were cultured under standard conditions. Cell lysates were dissolved in SDS-sample buffer, followed by immunoblot analysis using anti-SUMO-2/3 antibody. To confirm whether cellular proteins were equally blotted on each membrane, the membranes were re-probed with anti-tubulin antibody (lower panel). The positions of protein size markers are shown at left. (C) Non-transfected HEK293 cells (upper panel) and FLAG-mNip45 cells (lower panel) were cultured under standard conditions and subjected to indirect-immunofluorescence assays using anti-FLAG (left) and SUMO-2/3 (center) antibodies. DAPI staining was used for nuclear staining (right panel). Bar indicates 20 μ m. (D) The SUMO-2/3 nuclear foci were quantified; cell numbers shown are the mean \pm standard deviation (SD) of three independent experiments (* $p < 0.05$ by Student's *t*-test). White bars represent the values of non-transfected cells; black bars, FLAG-mNip45 expressing cells.

Sekiya et al. have reported the crystal structures of mNip45-SLD2, both in free form and complexed with an E2 SUMO-conjugating enzyme, Ubc9. They showed that mNip45-SLD2 binds to Ubc9 in a manner almost identical to that of SUMO paralogs, SUMO-1 and SUMO-2/3 (see Fig. 1A) [11]. It has also been reported that the SLDs of Rad60, a Nip45 homolog in the fission yeast *Schizosaccharomyces pombe*, interacts with Ubc9 [12]. Comparison of structural data between mNip45-SLD2:Ubc9 and Rad60-SLD2:Ubc9 complexes suggests that the interaction between RENi family members and Ubc9 appears to be evolutionarily conserved [11–13], arguing that RENi proteins act as SUMO-stable fusion proteins mimicking SUMO. Although it has been shown that mNip45-SLD2 inhibits *in vitro* elongation of SUMO chains, whether Nip45 confers such an inhibitory effect on the polymerization of SUMOs *in vivo* remains unclear. In addition, in contrast to the C-terminal region of Nip45, the N-terminal region is poorly characterized.

In this study, we established a human cell line, in which FLAG-tagged mouse Nip45 (FLAG-mNip45) was stably overexpressed. Using this cell line, the involvement of Nip45 with the metabolism of SUMO/SUMOylated proteins in response to proteasome inhibition was revealed. We also found that the N-terminal region of Nip45 has the potential to interact with SUMO-3 and SUMO-2/3 chains, which explains one *in vivo* action of Nip45. Our study provides novel information on a poorly characterized mammalian protein and suggests that our newly established cell line will be useful for elucidating the physiological role of Nip45.

2. Materials and methods

2.1. Plasmids

To generate Nip45 expression vectors, mNip45 cDNA was amplified by polymerase chain reaction (PCR) using appropriate primers (primer sequences available upon request). The generated PCR fragments were cloned into pET28 (Novagen), pGEX 4T-1 (GE Healthcare), and pcDNA3 (Invitrogen). The deletion mutants of mNip45 were also generated by PCR. SUMO-1/2/3 expression plasmids were used as described previously [14,15].

2.2. Antibodies

Two rat monoclonal antibodies, against SUMO-2/3 and against SUMO-1, were described previously [14]. The other antibodies used in this study were anti-SUMO-1, anti-SUMO-2/3, anti-Ubc9 (Cell signaling TECHNOLOGY and BD), anti-Nip45, anti-His₆, anti-GST, anti- γ -tubulin, anti-PML (Santa Cruz Biotechnology), anti-K48/K63-specific ubiquitin (Millipore), and anti-FLAG M2 (Sigma-Aldrich).

2.3. Recombinant protein expression and GST-pull-down assay

Expression of recombinant proteins and purifications of GST fusion proteins and His₆ fusion proteins were carried out as previously described [14]. Standard conditions were as follows: bacterially expressed GST and GST fusion proteins were immobilized on glutathione-Sepharose beads (GE healthcare), and were incubated with lysate prepared from either *Escherichia coli* in phosphate-buffered saline (PBS) containing 0.1% Triton X-100. Proteins associated with the beads were analyzed by sodium dodecyl sulfate (SDS)-PAGE, followed by immunoblot analysis [14,15]. Poly-ubiquitin chains (ubi_{1–7}-K48- and -K63-linked) were purchased from Boston Biochem.

2.4. Generation of SUMO-3 chains in bacterial SUMOylation system

Recombinant SUMO-3 chains were obtained using an *E. coli* SUMOylation system [16,17]. Briefly, *E. coli* strain BL21 (DE3) co-transformed with pET28-SUMO-3 and pT-E1E2S3 protein expression vectors was used to express His₆-tagged SUMO-3 that was modified SUMO-3, designated as SUMO-3 chains. Expression of recombinant proteins was induced with 0.2 mM isopropyl β -D-galactopyranoside (IPTG) at 25 °C for 18 h. This procedure to express SUMO chains in bacteria have been also used by other groups [18,19].

2.5. Cell culture and transfection

Human embryonic kidney 293 (HEK293) cells were cultured in Dulbecco's modified Eagle's medium nutrient mixture F-12 Ham with 5% fetal calf serum and antibiotics, in 5% CO₂. MG132 (Sigma–Aldrich/Peptide Institute) was dissolved in dimethyl sulfoxide (DMSO) and added to culture medium as indicated in the text. Cells were transfected with plasmid DNAs by X-tremeGENE HP transfection reagent (Roche), according to the manufacturer's protocol.

2.6. Establishment of FLAG-mNip45 stable expression cell line

The Flp-In HEK293 cell line (Invitrogen), which contains a Flp recombination target (FRT) site in its genome, was maintained in Dulbecco's modified Eagle's medium with 10% fetal calf serum, 1% penicillin and streptomycin, 2 mM L-glutamine (Sigma–Aldrich), 200 μ g/ml zeocin, and 15 μ g/ml blasticidin S (Invitrogen). To establish the mNip45 stable expression HEK293 cells, pcDNA5/FRT/V5-His-TOPO vectors encoding wild-type mNip45 and pOG44 vector (Invitrogen), which expresses Flp recombinase, were cotransfected at a molar ratio of 1:9 into Flp-In 293 cells. After 48 h post transfection, hygromycin B (200 μ g/ml; Invitrogen) was added to the culture for selection. After 2 weeks, hygromycin-resistant cells were harvested and several colonies were selected. One of the selected colonies was used for the further analysis described in the text.

2.7. Indirect immunofluorescence assay

Cultured cells grown on glass coverslips were fixed with 4% paraformaldehyde in PBS for 15 min at room temperature. Then cells were permeabilized with 0.5% Triton X-100 in PBS for 5 min on ice. After the permeabilization, cells were blocked in 0.2% BSA, 0.1% Triton X-100 in PBS for 20 min and incubated with primary antibody for 1 h, followed by an appropriate secondary antibody. The coverslips were mounted on slide glasses using glycerol–DABCO (Wako Pure Chemical Industries) and samples were analyzed with a DP72 microscope (Olympus). DNA was visualized with 4',6-diamidino-2-phenylindole (DAPI).

2.8. Immunoprecipitation and immunoblot analysis

Cultured cells were rinsed with PBS and lysed with 1% Triton X-100 buffer (20 mM Hepes–NaOH (pH 7.5), 1% Triton X-100, 300 mM NaCl, 10 mM MgCl₂, 2 mM NaF, 20 mM N-ethylmaleimide (NEM), 0.1 mM dithiothreitol (DTT), 10% glycerol, and the protease inhibitors (Sigma–Aldrich) on ice for 30 min. After centrifugation at 20,000 g for 15 min, supernatant were subjected to appropriate antibodies that was pre-bound to protein G beads (GE Healthcare) and rotated for 1 h at 4 °C. After rotation, the beads were washed with 1% Triton X-100 buffer 3 times. Immunoblot analysis was carried out as described previously [14,15].

3. Results and discussion

3.1. Establishment of HEK293 cells expressing FLAG-mNip45

To investigate the *in vivo* function of Nip45, we endeavored to analyze endogenously expressed Nip45 in cultured human cells using specific antibodies. Unfortunately, neither our newly generated nor commercially available Nip45 antibodies showed sufficient sensitivity to enable such an approach. To circumvent this problem, a HEK293 cell line stably expressing FLAG-epitope-tagged full-length mNip45 (FLAG-mNip45) was generated (see Section 2). Based on the immunoblot analysis shown in Supplementary Fig. 1A and B, FLAG-mNip45 was expressed at levels approximately 13 times higher than those of endogenous Nip45. When the cells, cultured under standard, non-stressful conditions, were subjected to indirect-immunofluorescence analysis, anti-FLAG antibody detected prominent signals throughout the nucleus without any detectable foci, but detected no signals in non-transfected HEK293 cells (Supplementary Fig. 1C). These results indicate that Nip45 can be detectable in the newly established FLAG-mNip45 expressing cells, facilitating the biochemical and cell biological analysis of Nip45 in a mammalian cell culture system.

3.2. Formation of nuclear SUMO-2/3-foci, but not accumulation of SUMOylated proteins, is correlated with Nip45 expression

mNip45-SLD2 inhibits elongation of polymerization of SUMOs (SUMO-chain formation) *in vitro* [11]. Therefore, overexpression of FLAG-mNip45 in mammalian cells may cause a dramatic reduction in the level of SUMOylated proteins owing to an excess of the C-terminal moiety that inhibits the activity of Ubc9. Thus, we wished to use this newly established cell line to investigate whether FLAG-mNip45 interacted with Ubc9 via its C-terminal SLD2 to produce an inhibitory effect on SUMOylation. To this end, we performed immunoprecipitation (Supplementary Fig. 2) and immunoblot analyses (Fig. 1B). However, contrary to our expectations, we were unable to show interaction between full-length FLAG-mNip45 and Ubc9 in the immunoprecipitation experiment (lane 1 of FL in Supplementary Fig. 2). Moreover, immunoblot analysis showed that the amount of higher molecular mass SUMOylated proteins in FLAG-mNip45 expressing cells was not different from that in non-transfected cells (Fig. 1B), suggesting a negligible effect of FLAG-mNip45 expression on global SUMOylation. Similar data were obtained when we used HEK293 cells in which FLAG-mNip45 was transiently transfected and overexpressed (Supplementary Fig. 2 and data not shown). These results indicate that, in contrast to *in vitro* experiments [11], Nip45 could not stably interact with Ubc9 and thus could not effectively inhibit polySUMOylation *in vivo*, suggesting that the SLD2 binding surface for Ubc9 in the full-length FLAG-mNip45 is protected by an unknown mechanism in the cultured cells.

It should be noted that, during the course of establishing the cell line, indirect-immunofluorescence assays using anti-SUMO-2/3 antibody revealed that cells expressing FLAG-mNip45 showed increased numbers of discrete SUMO-2/3-foci in the nucleus compared with non-transfected HEK293 cells (Fig. 1C and D). As stated above, immunoblots probed with anti-SUMO-2/3 antibody revealed negligible alteration of the global SUMOylation pattern in FLAG-mNip45 expressing cells compared with that in non-transfected cells (Fig. 1B). This indicated that Nip45 overexpression may affect the metabolism of SUMOylated proteins, possibly by altering targeting/deposition of SUMOylated proteins in the nucleus, but not by inhibiting global SUMOylated proteins *per se*.

3.3. Proteasome inhibition leads to colocalization of Nip45 with SUMO-2/3 at PML bodies

The level of SUMOylated proteins is dramatically increased in response to certain environmental stimuli and proteasome inhibition by MG132 leads to the accumulation of SUMOylated proteins at discrete foci in the nucleus, in the proximity to promyelocytic leukemia (PML) bodies [20–23]. The molecular mechanism underlying this process remains largely uninvestigated. We considered that Nip45 might affect the process; therefore, we assessed the association between Nip45 and the SUMO pathway in our cell line.

As shown in Fig. 2A and B, MG132 induced the accumulation of SUMOylated proteins and increased the number of nuclear SUMO-2/3 foci associated with PML bodies from approximately 0–2 to 6–12 per cell in FLAG-mNip45 expressing HEK293 cells. This suggested that the cell line had the potential to respond to proteasome inhibition in a similar manner to that observed in other human cells [20–23]. We then determined the effect of MG132 treatment on Nip45 subcellular localization. In the immunofluorescence analysis shown in Fig. 2B and C, the anti-FLAG antibody barely detected foci in the absence of MG132; however, in the presence of MG132, the number of foci detectable with anti-FLAG antibody increased from approximately 0–1 to 3–5 per cell, suggesting that Nip45 has the potential to accumulate at/around subnuclear structures in response to proteasome inhibition. Importantly, most, but not all, of the foci were co-stained with anti-SUMO-2/3 antibody and appeared to be closely associated with nuclear domains detected by anti-PML antibody (Fig. 2B), indicating that a significant portion of FLAG-mNip45 was associated with SUMO/SUMOylated proteins at/around PML bodies in response to proteasome inhibition by MG132.

3.4. Nip45 is not efficiently SUMOylated

It is possible that proteasome inhibition could induce SUMOylation of Nip45 itself, resulting in co-staining of the two independently translated FLAG-mNip45 and SUMO-2/3 proteins at the nuclear foci. Thus we elucidated whether Nip45 was SUMOylated in the presence or absence of MG132. As shown in Fig. 3A, when the proteins immunoprecipitated with anti-FLAG antibody were probed with anti-FLAG antibodies, no band with a higher molecular weight than full-length FLAG-mNip45 was detected in either dimethyl sulfoxide (DMSO)- or MG132-treated cells. More than 95% of the total cellular pool of FLAG-mNip45 could be extracted, both in the presence or absence of MG132 (data not shown), indicating that FLAG-mNip45 is modified very poorly, if at all, by SUMO either in the presence or absence of proteasome inhibition. Furthermore, bacterially expressed GST-mNip45 was SUMOylated very inefficiently in a bacterial SUMOylation system, whereas a large amount of RanBP2-IR fragment, a well-known SUMO-E3 ligase and efficient SUMO substrate [24], was SUMOylated under the same conditions (Fig. 3B), supporting the notion that Nip45 is a very poor SUMOylation substrate.

3.5. Identification of Nip45 as a SUMO-binding protein

Our data suggested an interaction between Nip45 and the SUMO pathway, not simply *via* direct interaction with Ubc9 to inhibit global SUMOylation, but *via* close association with SUMO/SUMOylated proteins especially when treated with proteasome inhibitor. To elucidate the role of Nip45 in the regulation of SUMO/SUMOylated proteins, we tested whether Nip45 can directly interact with SUMO using recombinant mNip45 and its deletion

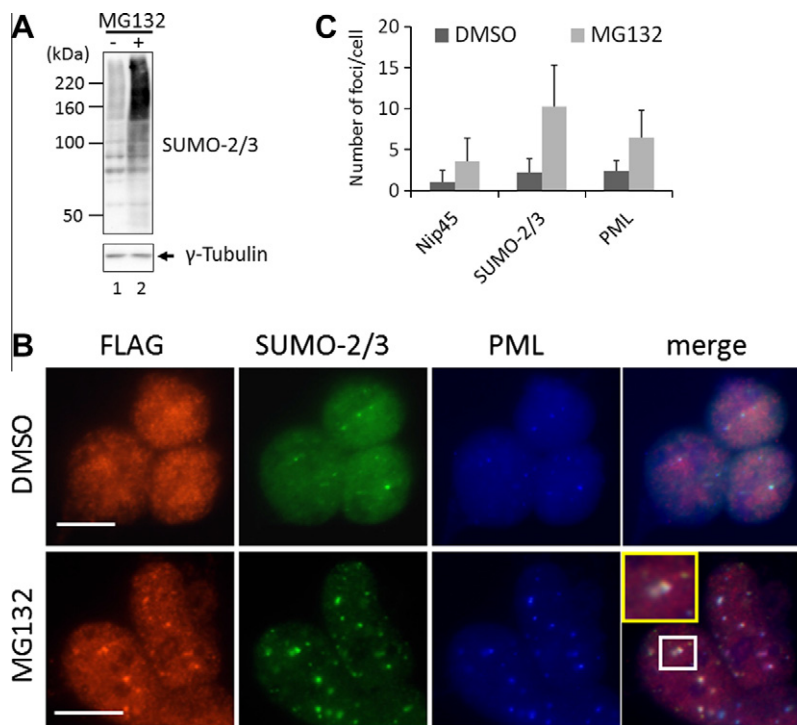


Fig. 2. Effect of proteasome inhibition by MG132 on subcellular localization of Nip45. (A) FLAG-mNip45 expressing cells were treated with DMSO alone (–MG132; lane 1) or MG132 (20 μ M, +MG132; lane 2) for 5 h and were harvested. Total cell lysates were subjected to SDS–PAGE, followed by immunoblot analysis for detection of SUMO-2/3 (upper panel), γ -tubulin (middle panel), and Ubc9 (bottom panel). (B) Exponentially growing FLAG-mNip45 expressing cells were treated with MG132 (20 μ M, +MG132) or DMSO alone (–MG132) for 5 h and subjected to indirect-immunofluorescence assays. Cells were double-stained with anti-FLAG (left) and anti-SUMO-2/3 antibodies (upper panel), or with anti-FLAG and anti-PML antibodies (bottom panel). In each assay, merged images are shown at right. An inset (yellow) in the right-bottom picture shows a 2-fold magnification of a selected region (white). Bar indicates 20 μ m. (C) The number of FLAG-mNip45 foci as well as SUMO-2/3- and PML-foci were quantified. The numbers shown are the means \pm standard deviation (SD) of three independent experiments (* p < 0.05 by Student's t -test). Gray bars represent DMSO-treated cells. Black bars show MG132-treated cells. (For interpretation of the references to color in this figure legend, the reader is referred to the web version of this article.)

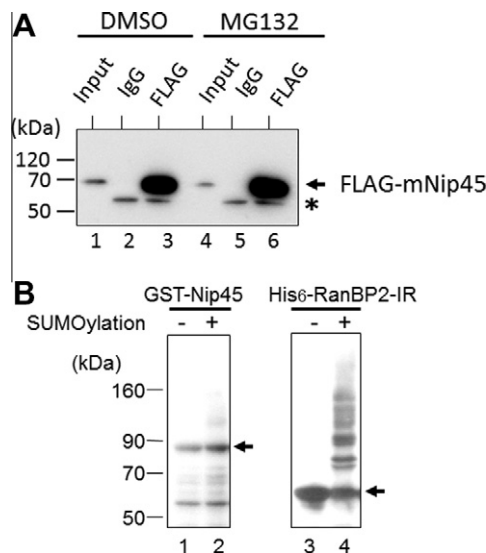


Fig. 3. Nip45 is not efficiently SUMOylated. (A) FLAG-mNip45 expressing cells were treated with DMSO alone or with MG132 (20 μ M) for 5 h and then harvested. Cell lysates were prepared from DMSO-treated (lanes 1, 2 and 3) and MG132-treated (lanes 4, 5 and 6) cells, followed by immunoprecipitation assays using control IgG (lanes 2 and 4) or anti-FLAG (lanes 3 and 6) antibody. Immunoprecipitated fractions were subjected to immunoblot analysis using anti-FLAG antibody. Aliquots of total cell lysate used for each experiment are shown as ‘input’ in lanes 1 and 4. The arrow indicates the position of FLAG-mNip45 at approximately 70 kDa. Asterisk (*) indicates the position of non-specific bands at approximately 60 kDa, possibly IgG-heavy chain. Molecular size markers are indicated at left. (B) GST-mNip45 (lanes 1 and 2) and His₆-RanBP2-IR (lanes 3 and 4) proteins were subjected to either bacterial SUMOylation (+; lanes 2 and 4) or to a standard bacterial expression (–; lanes 1 and 3) system, followed by purification with glutathione Sepharose beads for GST-mNip45 or N2*i*-beads for His₆-RanBP2-IR. Purified products were subjected to immunoblot analysis and probed with anti-GST antibody or anti His₆-antibody. Molecular size markers are indicated at left. Arrows indicate the positions of non-modified forms of GST-Nip45 and His₆-RanBP2-IR, respectively.

mutants (Fig. 1A and Supplementary Fig. 3). As shown in Fig. 4A and B, GST-full-length mNip45 (FL) and GST-N-terminal region (NT), and to lesser extent GST-C-terminal region (CT), GST-SLD1 (C1), GST-SLD2 (C2), and GST-alone, bound efficiently to His₆-SUMO-3 and polySUMO-3 chains. This indicated the ability of the N-terminal region to interact directly with SUMO/SUMO chains. It is probable that Nip45 does not bind Ub chains *in vitro* given that no interaction between GST-Nip45 constructs and Ub 48 or Ub 63 chains was detected in the GST-pulldown assay (Supplementary Fig. 4). Therefore, we conclude that Nip45 has the potential to interact with both SUMO and SUMO chains, but not with Ub/Ub chains, via its N-terminal region. In addition, as shown in Fig. 4C, a comparison of the N-terminal regions of mNip45 and hNip45 revealed at least four highly conserved amino acid sequences similar to the canonical SUMO-interacting/-binding motif (SIM/SBM) [14,15,25]. In *S. pombe* a homolog of Nip45, Rad60, has been predicted to contain multiple SIMs (two are in the N-terminal domain and the others are in the C-terminal domain); however, the SUMO-binding ability of Rad60 has not been tested experimentally [26]. Thus, this study is the first to experimentally show that a RENI family protein is a SUMO-interacting protein.

In summary, using our newly established FLAG-mNip45 expressing cells, we have shown that Nip45 is localized in the nucleus under non-stressful conditions, while during proteasome inhibition, Nip45 accumulates at SUMO-containing nuclear foci associated with PML bodies. The direct interaction of the N-terminal region of Nip45 with SUMO and SUMO chains *in vitro* suggest a previously unknown association of a mammalian RENI family protein with the SUMO pathway. Indeed, it may be feasible that Nip45

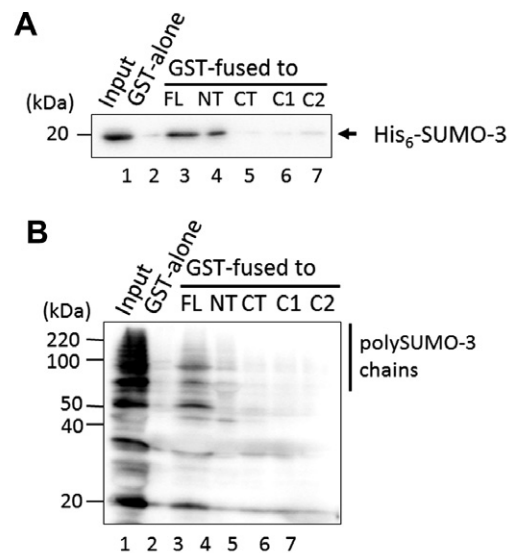


Fig. 4. Nip45 is a SUMO-interacting protein. (A) Interaction of His₆-SUMO-3 with GST-Nip45 and the set of recombinant deletion proteins. Aliquots (500 μ l) of bacterial lysate containing His₆-SUMO-3 were incubated with beads bound to 3 μ g of GST-alone (lane 2) or GST-fusion proteins as indicated in the figure (lanes 3, 4, 5, 6, and 7). Following incubation, proteins associated with the beads were subjected to immunoblot analysis using anti-His₆ antibody. Bacterial lysate (5% of input) was loaded on lane 1. The position of His₆-SUMO-3 (20 kDa) is indicated by the arrowhead. (B) Interaction of bacterially expressed SUMO-3 chains with GST-Nip45 and the set of recombinant deletion proteins. Aliquots (500 μ l) of bacterial lysate containing SUMOylated His₆-SUMO-3 proteins were incubated with beads bound to 3 μ g of GST-alone (lane 2) or to GST-fusion proteins as indicated in the figure (lanes 3, 4, 5, 6, and 7). Following incubation, proteins associated with the beads were subjected to immunoblot analysis using a SUMO-2/3 antibody. Bacterial lysate (5% of input) was loaded on lane 1. The vertical line on the right side represents SUMO-3 chains. The positions of protein size markers are shown at left. (C) Sequence comparison of putative SUMO-interacting motifs in mouse and human Nip45. The numbers correspond to the amino acid residues in mNip45 (upper) and hNip45 (lower).

functions as a recipient of SUMO/SUMOylated proteins in the context of assembly and/or disassembly of SUMOylated proteins around PML bodies in response to proteasome inhibition. Since we found that full-length Nip45 does not stably interact with Ubc9 in cells, further analysis is required to establish its functional linkage with Ubc9 *in vivo*. The cell line described here, which constitutively expresses a tagged version of Nip45, will facilitate analysis of Nip45 function in the nucleus.

Acknowledgments

We thank Drs. Tokio Tani and Takeshi Kitano of the Department of Biological Sciences, Kumamoto University for valuable suggestions and discussion. We also thank Mr. William Berge for reading the manuscript. This work was supported by JSPS KAKENHI Grant Number 23616004 and MEXT KAKENHI Grant Number 23131519.

Appendix A. Supplementary data

Supplementary data associated with this article can be found, in the online version, at <http://dx.doi.org/10.1016/j.bbrc.2012.11.020>.

References

- [1] M.R. Hodge, H.J. Chun, J. Rengarajan, A. Alt, R. Lieberson, L.H. Glimcher, NF-AT-Driven interleukin-4 transcription potentiated by NIP45, *Science* 274 (1996) 1903–1905.
- [2] R. Lieberson, K.A. Mowen, K.D. McBride, V. Leautaud, X. Zhang, W.K. Suh, L. Wu, L.H. Glimcher, Tumor necrosis factor receptor-associated factor (TRAF)2 represses the T helper cell type 2 response through interaction with NFAT-interacting protein (NIP45), *J. Exp. Med.* 194 (2001) 89–98.
- [3] A.F. Cunningham, M. Khan, J. Ball, K.M. Toellner, K. Serre, E. Mohr, I.C. MacLennan, Responses to the soluble flagellar protein FltC are Th2, while those to FltC on Salmonella are Th1, *Eur. J. Immunol.* 34 (2004) 2986–2995.
- [4] P.J. Bryce, M.K. Oyoshi, S. Kawamoto, H.C. Oettgen, E.N. Tsitsikov, TRAF1 regulates Th2 differentiation, allergic inflammation and nuclear localization of the Th2 transcription factor, NIP45, *Int. Immunol.* 18 (2006) 101–111.
- [5] J.W. Fathman, M.F. Gurish, S. Hemmers, K. Bonham, D.S. Friend, M.J. Grusby, L.H. Glimcher, K.A. Mowen, NIP45 controls the magnitude of the type 2 T helper cell response, *Proc. Natl. Acad. Sci. USA* 107 (2010) 3663–3668.
- [6] S. Shanmugarajan, C.J. Haycraft, S.V. Reddy, W.L. Ries, NIP45 negatively regulates RANK ligand induced osteoclast differentiation, *J. Cell Biochem.* 113 (2012) 1274–1281.
- [7] K.A. Mowen, B.T. Schurter, J.W. Fathman, M. David, L.H. Glimcher, Arginine methylation of NIP45 modulates cytokine gene expression in effector T lymphocytes, *Mol. Cell* 15 (2004) 559–571.
- [8] M. Novatchkova, A. Bachmair, B. Eisenhaber, F. Eisenhaber, Proteins with two SUMO-like domains in chromatin-associated complexes: The RENi (Rad60-Esc2-NIP45) family, *BMC Bioinformatics* 6 (2005) 22.
- [9] I.B. Kuznetsov, S. Rackovsky, On the properties and sequence context of structurally ambivalent fragments in proteins, *Protein Sci.* 12 (2003) 2420–2433.
- [10] J. Liu, H. Tan, B. Rost, Loopy proteins appear conserved in evolution, *J. Mol. Biol.* 322 (2002) 53–64.
- [11] N. Sekiyama, K. Arita, Y. Ikeda, K. Hashiguchi, M. Ariyoshi, H. Tochio, H. Saitoh, M. Shirakawa, Structural basis for regulation of poly-SUMO chain by a SUMO-like domain of Nip45, *Proteins* 78 (2010) 1491–1502.
- [12] J. Prudden, J.J. Perry, A.S. Arvai, J.A. Tainer, M.N. Boddy, Molecular mimicry of SUMO promotes DNA repair, *Nat. Struct. Mol. Biol.* 16 (2009) 509–516.
- [13] J. Prudden, J.J. Perry, M. Nie, A.A. Vashisht, A.S. Arvai, C. Hitomi, G. Guenther, J.A. Wohlschlegel, J.A. Tainer, M.N. Boddy, DNA repair and global SUMOylation are regulated by distinct Ubc9 noncovalent complexes, *Mol. Cell. Biol.* 31 (2011) 2299–2310.
- [14] Y. Uchimura, T. Ichimura, J. Uwada, T. Tachibana, S. Sugahara, M. Nakao, H. Saitoh, Involvement of SUMO modification in MBD1- and MCAF1-mediated heterochromatin formation, *J. Biol. Chem.* 281 (2006) 23180–23190.
- [15] J. Uwada, N. Tanaka, Y. Yamaguchi, Y. Uchimura, K. Shibahara, M. Nakao, H. Saitoh, The p150 subunit of CAF-1 causes association of SUMO2/3 with the DNA replication foci, *Biochem. Biophys. Res. Commun.* 391 (2010) 407–413.
- [16] Y. Uchimura, M. Nakamura, K. Sugawara, M. Nakao, H. Saitoh, Overproduction of eukaryotic SUMO-1- and SUMO-2-conjugated proteins in *Escherichia coli*, *Anal. Biochem.* 331 (2004) 204–206.
- [17] H. Saitoh, J. Uwada, K. Azusa, Strategies for the expression of SUMO-modified target proteins in *Escherichia coli*, *Methods Mol. Biol.* 497 (2009) 211–221.
- [18] M. Békés, J. Prudden, T. Srikumar, B. Raught, M.N. Boddy, G.S. Salvesen, The dynamics and mechanism of SUMO chain deconjugation by SUMO-specific proteases, *J. Biol. Chem.* 286 (2011) 10238–10247.
- [19] M. Nie, A. Aslanian, J. Prudden, J. Heideker, A.A. Vashisht, J.A. Wohlschlegel, J.R. Yates, M.N. Boddy, Dual recruitment of Cdc48 (p97)-Ufd1-Npl4 by SUMO and ubiquitin in STUbL-mediated genome stability functions, *J. Biol. Chem.* 287 (2012) 29610–29619.
- [20] D. Bailey, P. O'Hare, Comparison of the SUMO1 and ubiquitin conjugation pathways during the inhibition of proteasome activity with evidence of SUMO1 recycling, *Biochem. J.* 392 (2005) 271–281.
- [21] J. Schimmel, K.M. Larsen, I. Matic, M. van Hagen, J. Cox, M. Mann, J.S. Andersen, A.C. Vertegaal, The ubiquitin-proteasome system is a key component of the SUMO-2/3 cycle, *Mol. Cell Proteom.* 7 (2008) 2107–2122.
- [22] M.H. Tatham, I. Matic, M. Mann, R.T. Hay, Comparative proteomic analysis identifies a role for SUMO in protein quality control, *Sci. Signal.* 4 (178) (2011) rs4.
- [23] M. Castorálová, D. Březinová, M. Svěda, J. Lipov, T. Ruml, Z. Knejzlík, SUMO-2/3 conjugates accumulating under heat shock or MG132 treatment result largely from new protein synthesis, *Biochim. Biophys. Acta* 1823 (2012) 911–919.
- [24] A. Pichler, P. Knipscheer, H. Saitoh, T.K. Sixma, F. Melchior, The RanBP2 SUMO E3 ligase is neither HECT- nor RING-type, *Nat. Struct. Mol. Biol.* 11 (2004) 984–991.
- [25] C.M. Hecker, M. Rabiller, K. Haglund, P. Bayer, I. Dikic, Specification of SUMO1- and SUMO2-interacting motifs, *J. Biol. Chem.* 281 (2006) 16117–16127.
- [26] L.K. Boyd, B. Mercer, D. Thompson, E. Main, F.Z. Watts, Characterisation of the SUMO-like domains of *Schizosaccharomyces pombe* Rad60, *PLoS ONE* 5 (2010) e13009.